The Journal of Chemical Physics | COMMUNICATION | scitation.org/journal/jcp

N-WASP is competent for downstream signaling before full release from autoinhibition

Cite as: J. Chem. Phys. 158, 091105 (2023); doi: 10.1063/5.0137908
Submitted: 6 December 2022 • Accepted: 13 February 2023 •
Published Online: 7 March 2023

Souvik Dey[1] and Huan-Xiang Zhou[1,2,a)]

AFFILIATIONS

[1] Department of Chemistry, University of Illinois at Chicago, Chicago, Illinois 60607, USA
[2] Department of Physics, University of Illinois at Chicago, Chicago, Illinois 60607, USA

Note: This paper is part of the JCP Special Topic on New Views of Allostery.
[a)]**Author to whom correspondence should be addressed:** hzhou43@uic.edu

ABSTRACT

Allosteric regulation of intrinsically disordered proteins (IDPs) is still vastly understudied compared to the counterpart of structured proteins. Here, we used molecular dynamics simulations to characterize the regulation of the IDP N-WASP by the binding of its basic region with inter- and intramolecular ligands (PIP_2 and an acidic motif, respectively). The intramolecular interactions keep N-WASP in an autoinhibited state; PIP_2 binding frees the acidic motif for interacting with Arp2/3 and thereby initiating actin polymerization. We show that PIP_2 and the acidic motif compete in binding with the basic region. However, even when PIP_2 is present at 30% in the membrane, the acidic motif is free of contact with the basic region ("open" state) in only 8.5% of the population. The very C-terminal three residues of the A motif are crucial for Arp2/3 binding; conformations where only the A tail is free are present at a much higher population than the open state (40- to 6-fold, depending on the PIP_2 level). Thus, N-WASP is competent for Arp2/3 binding before it is fully freed from autoinhibition.

Allostery is a concept traditionally applied to structured proteins such as hemoglobin.[1] However, the interactions of intrinsically disordered proteins (IDPs) or regions (IDRs) with ligands in many respects have similar behaviors to the counterparts of structured proteins. For example, similar to hemoglobin binding of oxygen, IDRs interact with multiple copies of the same ligand, as illustrated by multisite phosphorylation[2] and by binding of multiple PIP_2 molecules.[3] Allostery in IDPs is still vastly understudied (see Ref. 4 for a recent review), and traditional ideas about allostery may well need modification. Most notably, whereas orthosteric and allosteric sites are well-defined and clearly separated in structured proteins, the binding of IDRs with ligands is typically fuzzy and there may not be a clear separation between orthosteric and allosteric sites. Moreover, IDPs frequently have intramolecular ligands. Here, we report on how the competition between intra- and intermolecular interactions contributes to the activation of the neural Wiskott–Aldrich syndrome protein (N-WASP) by the acidic lipid phosphatidylinositol 4,5-bisphosphate (PIP_2). A unique observation is that downstream signaling, i.e., binding with Arp2/3, may start even before N-WASP is fully released from autoinhibition.

N-WASP is intrinsically disordered, with a C-terminal verprolin-central-acidic (VCA) region that binds G-actin (via two tandem V motifs) and Arp2/3 (via the CA motifs) to initiate actin polymerization.[5–8] The very C-terminal three residues of the A motif (the A tail) are crucial for Arp2/3 binding.[8,9] Under resting conditions, N-WASP is autoinhibited by intramolecular interactions between the C motif and an upstream GTPase-binding domain (GBD),[7,10–12] and between the A motif and a basic region (BR) preceding the GBD[13–15] [Fig. 1(a)]. The binding of the small GTPase Cdc42 to the GBD displaces the C motif, whereas the binding of PIP_2 to the BR displaces the A motif, and these two ligands synergistically activate N-WASP.[3,7,12,16,17] In our previous study, we used molecular dynamics (MD) simulations to characterize the activated state, where N-WASP is simultaneously bound to a PIP_2-containing membrane and Cdc42.[18] Here, we wanted to understand the activation process induced by PIP_2 binding and, in particular, to characterize the N-WASP conformations competent for Arp2/3 binding.

We started with building a structural model for N-WASP in the autoinhibited state [Fig. 1(a)]. For the intramolecular complex

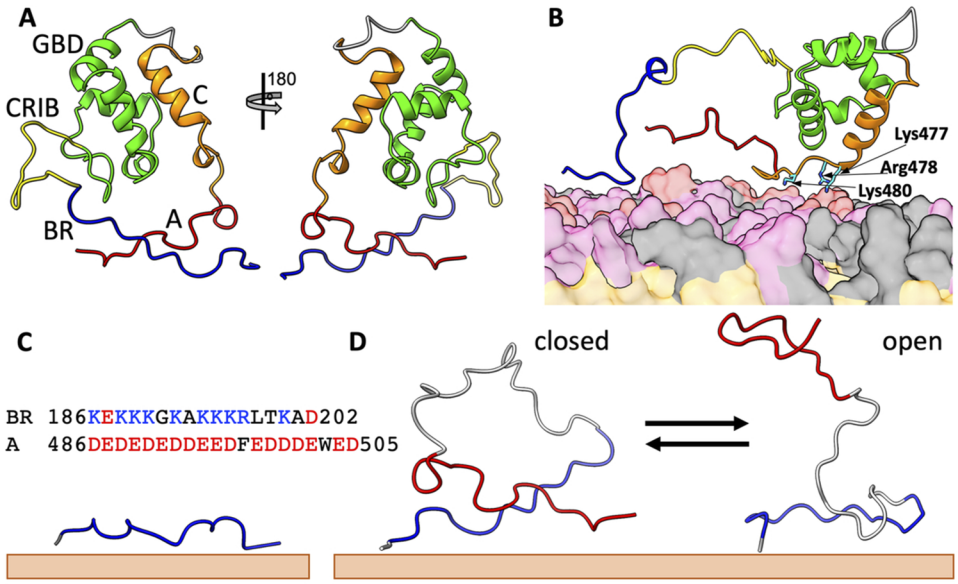

FIG. 1. Structures of N-WASP in different states. (a) Autoinhibited state. The C-terminal central ("C") motif forms a helix and is docked to the GTPase-binding domain (GBD), whereas the C-terminal acidic ("A") motif locks with the basic region (BR) in a cross-arm pose. Note that, following the construct for the NMR structure 1EJ5,[11] residues between the GBD (ending with Gln275) and the C motif (starting with Ala462) were replaced by a six-residue linker [sequence $(GGS)_2$]. The N-terminal 185 residues (preceding the start of the BR at Lys186) were also not included. (b) An intermediate upon activation by PIP_2. The A motif is released from the BR, but the C motif is still bound to the GBD, and three basic residues between the C-motif helix and the A motif bind to the membrane and keep the A motif in proximity to the BR. (c) A membrane-bound BR-only fragment. The sequences of the BR and the A motif are also shown. (d) A BR-A fragment undergoing closed-to-open transition on the membrane surface. BR, CRIB, GBD, C, and A are in blue, yellow, green, orange, and red, respectively; linkers are in gray. Lipids are shown as surface, with PIP_2, PS, and PC headgroups in red, pink, and gray, respectively; lipid tails are in orange.

between the GBD and the C motif, which forms an α-helix, we used homology modeling with the template from an NMR structure for the WASP counterpart (Protein Data Bank entry 1EJ5[11]). This complex places the BR and A motif on opposite sides; thus, we modeled their complex as a cross-arm pose. We put this autoinhibited structure at the surface of a membrane containing 10% PIP_2 to start four replicate MD simulations (each for 300 ns). PIP_2 was able to displace the A motif from the BR [Fig. 1(b)]. However, three basic residues, Lys477, Arg478, and Lys480, between the C-motif helix and the A motif are tethered to the membrane, thereby keeping the A motif in proximity to the BR.

To characterize its membrane binding free of interference by the rest of N-WASP, we carried out MD simulations of a BR-only fragment {residues 185–202, comprising the BR sequence [Fig. 1(c) inset] and an N-terminal Thr185} binding to membranes containing different levels of PIP_2 [Fig. 1(c)]. Experimentally, the BR-only fragment was found to bind with PIP_2-containing membranes.[3] To characterize the full dissociation of the A motif from the BR on the membrane surface, again without interference by the rest of N-WASP, we simulated a "BR-A" fragment, where the BR is connected to the A motif [sequence in Fig. 1(c) inset] by a 20-residue linker [with sequence $(GS)_{10}$], at membrane surfaces with a range of PIP_2 levels [Fig. 1(d)]. The simulation protocol largely followed our recent studies of IDP-membrane association.[18–22] In particular, the force fields were AMBER ff14SB[23] for proteins, TIP4P-D[24] for water, and Lipid17[25] for lipids (see supplementary material for details). Each leaflet of the membranes contained 100 lipids, of which 0–30 were PIP_2, 20 were POPS, and the rest were POPC. The simulations were run in 8 and 12 replicates for BR-only and BR-A fragments, respectively, on GPUs using pmemd.cuda[26] for 500 ns each. In the simulations, both fragments transiently dissociated from the membranes and then quickly reassociated. The re-equilibration with membranes and a high number of replicates ensured convergence of the simulation results.

Figure 2(a) displays the membrane contact probabilities of the BR residues in the BR-only fragment when bound with membranes containing 0%, 2%, 3%, 5%, and 10% PIP_2. As expected, the membrane contact probabilities of individual BR residues increase with increasing PIP_2 levels. Figure 2(b) displays the membrane contact probabilities of BR residues in the BR-A fragment at the membrane surfaces with 0%, 5%, 10%, 15%, 20%, 25%, and 30% PIP_2, again showing elevated membrane association at higher PIP_2 levels. However, two major differences between BR-only and BR-A are observed. First, because of the competition between PIP_2 and the A motif for BR binding, a higher level of PIP_2 is required to reach a similar extent of BR-membrane association when the fragment contains an intramolecular ligand, i.e., the A motif.

Second, while the membrane contact probabilities rise uniformly across the BR sequence in the BR-only simulations, the rises are much more rapid in the first half of the BR sequence in the BR-A simulations. To quantify this difference between the two fragments, we added up the membrane contact probabilities over the

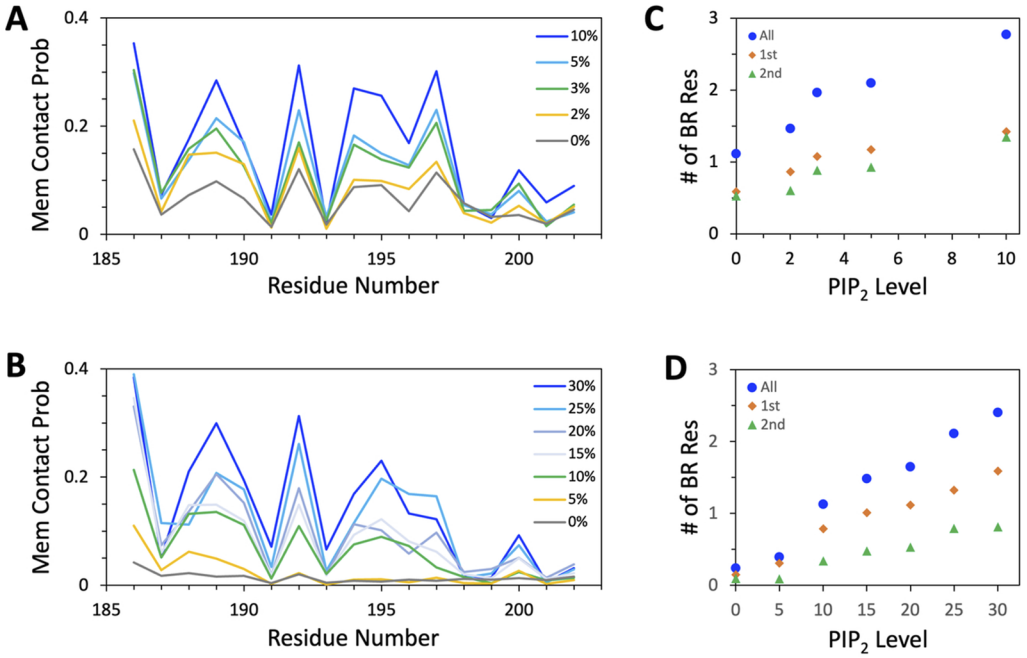

FIG. 2. Membrane binding properties of the BR-only and BR-A fragments. (a) Membrane contact probabilities of BR residues in the BR-only fragment at five PIP_2 levels. A membrane contact was formed when two heavy atoms, one from a given residue and one from any lipid, were within 3.5 Å. (b) Membrane contact probabilities of BR residues in the BR-A fragment at seven PIP_2 levels. (c) The mean number of BR residues in the BR-only fragment bound to a membrane at a given PIP_2 level. (d) The mean number of BR residues in the BR-A fragment bound to a membrane at a given PIP_2 level. All, 1st, and 2nd represent results calculated for the entire BR sequence or its first or second half.

first half (residues 186–193), the second half (residues 194–202), or the entire BR sequence. The sum in each case is the average number of BR residues in contact with the membrane at the same time. The results are shown in Fig. 2(c) for the BR-only fragment and in Fig. 2(d) for the BR-A fragment. Whereas the two halves make nearly equal contributions to the total number of membrane-contacting BR residues in the BR-only simulations, the first half makes double the contributions as the first half in the BR-A simulations.

Inter- and intramolecular interactions captured by snapshots from the MD simulations illustrate the above points and provide further insight. Figure 3(a) shows a representative snapshot from the BR-only simulations at 10% PIP_2. Four basic residues, Lys186, Lys194, Lys196, and Arg197, from across the entire BR sequence form salt bridges with a PIP_2, a PC, a PS, and a second PIP_2, respectively. The membrane-bound BR-A fragment samples a variety of poses, but of great interest are the ones where the A tail is free from BR engagement, as these poses are potentially competent for Arp2/3 binding. We distinguish two types of such poses: semi-open, where the A tail is free but the rest of the A motif could still be engaged with the BR; and open, where the entire A motif is freed from the BR. Figure 3(b) presents representative snapshots for the semi-open and open poses selected from the simulations at 30% PIP_2. In the semi-open pose shown in the left panel, Lys186, Lys189, and Lys192 in the first half of the BR sequence form salt bridges with two PIP_2 molecules. At the same time, Arg197 in the second half of the BR sequence forms salt bridges with Asp499 and Asp500 in the A motif. In the open pose, the A motif is fully released from the BR, and thus the interactions of the BR with the membrane are similar to those found for the BR-only fragment. In the snapshot in Fig. 3(b) right panel, Lys186, Lys189, Lys192, and Lys200 from across the entire BR sequence form salt bridges with two PIP_2 molecules. From here on, we restrict our attention to the BR-A fragment.

As illustrated in Fig. 3(b) left panel, the BR can engage with either PIP_2 or the A motif; hence, a rise in membrane-contacting BR residues is likely accompanied by a decline in A-contacting BR residues [Fig. 4(a)]. However, even at 30% PIP2, there are more BR residues engaged with the A motif (averaging 3.6 residues) than with lipids (averaging 2.4 residues). As acidic groups (17 Asp or Glu residues) in the A motif are vastly outnumbered by acidic lipids (30 PIP_2 and 20 POPS) in the simulations, the preference of the BR for intramolecular interactions is unequivocal. This preference can be explained by a high effective concentration afforded by covalently linking the BR and A motif.[27] The breakdown of the A-contacting BR residues shows that the second half of the BR sequence makes greater contributions than the first half [Fig. 4(a)], opposite to what is observed for membrane binding [Fig. 2(d)]. Therefore, the first half of the BR prefers PIP_2, whereas the second half prefers the A motif, as illustrated by Fig. 3(b) left panel. Combining inter- and intramolecular contacts, the total number of BR residues engaged is steady across different PIP_2 levels, with equal contributions from the two halves [Fig. 4(b)].

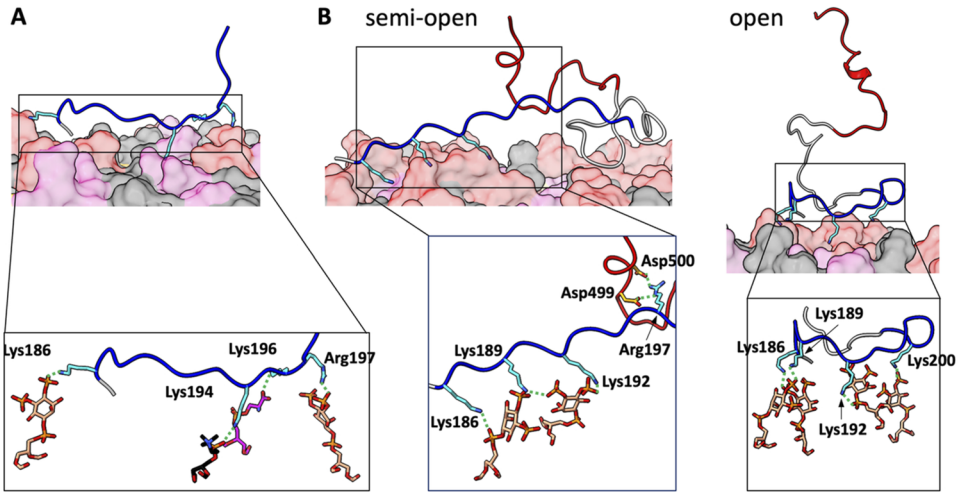

FIG. 3. Representative snapshots from MD simulations of membrane-bound BR-only and BR-A fragments. (a) BR-only fragment fully bound to a membrane with 10% PIP_2. (b) Two poses of the BR-A fragment bound to a membrane with 30% PIP_2. In the semi-open pose, the first half of the BR is engaged with the membrane, whereas the second half of the BR interacts with the A motif. In the open pose, the A motif is fully released from the BR. Sidechains that form membrane contacts are shown as sticks. In the zoomed images, the lipid partners are also shown as sticks, as are sidechains that form salt bridges between the BR and A motif. The coloring scheme is the same as in Fig. 1; carbon atoms in a stick representation follow the same coloring scheme, except that those in the BR and A motif are in cyan and orange, respectively; O, N, and P atoms are in red, blue, and orange, respectively.

So far, we have seen different behaviors of the two halves of the BR sequence in the competition between PIP_2 binding and A binding. A more important issue is the possible difference between the two halves of the A motif in BR engagement because the functionally important A tail resides in the second half. Figure 4(c) shows that the average number of BR-contacting A residues declines with increasing PIP_2 level; however, there are still 4.4 residues in the A motif engaged with the BR even at 30% PIP_2. Moreover, more of

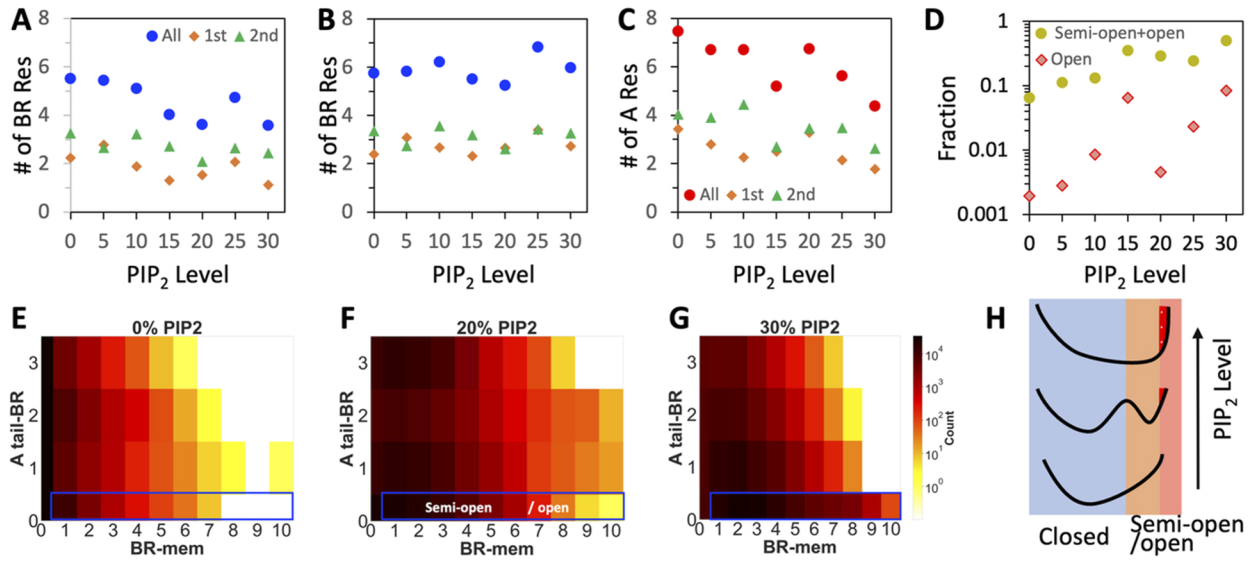

FIG. 4. Inter- and intramolecular binding properties of the BR-A fragments. (a) The mean number of BR residues bound to the A motif at a given PIP_2 level. (b) The mean total number of BR residues bound to either the membrane or the A motif at a given PIP_2 level. (c) The mean number of A-motif residues bound to the BR at a given PIP_2 level. In (a) and (b), All, 1st, and 2nd represent results calculated for the entire BR sequence or its first or second half; the meanings are similar in (c) except here the A-motif sequence is referenced. (d) Fraction of conformations in the semi-open (including open) state or the open state, as a function of PIP_2 level. (e)–(g) Two-dimensional histograms of conformations sampled at 0%, 20%, and 30% PIP_2. The blue box indicates the semi-open state; a sub-population in this box constitutes the open state. (h)Illustration of the changing energy landscape at increasing PIP_2 levels.

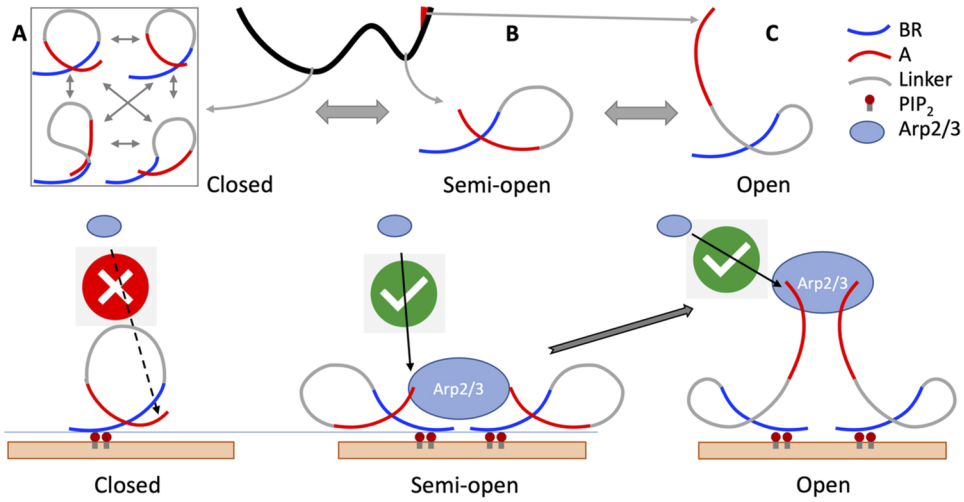

FIG. 5. The semi-open state as a functional rescue for downstream signaling. (a) N-WASP has the preponderance to stay closed and hence is unable to bind Arp2/3. (b) In the semi-open state, the freed A tail can engage with Arp2/3. This pre-engagement primes Arp2/3 to pull the A motif away from the BR, thereby creating a bypass to full binding. (c) N-WASP rarely samples the open state on its own.

these residues come from the second half than from the first half of the A motif.

The overwhelming preference of the BR for intramolecular interactions, especially with the second half of the A motif, does not bode well for N-WASP activation. Indeed, the population of the open state, where the entire A motif is freed from the BR, rises extremely slowly with increasing PIP_2 level, reaching only 8.5% even at 30% PIP_2 [Fig. 4(d)]. However, we recognize that N-WASP is already able to engage with Arp2/3 in the semi-open state. The semi-open population is significantly higher than the open population, by 40-fold at low PIP_2 but still 6-fold at 30% PIP_2, where the semi-open state accounts for 50% of the entire population [Fig. 4(d)].

To present a full view of the interplay between inter- and intramolecular interactions, we calculated two-dimensional histograms of the conformational ensemble at each PIP_2 level. The first coordinate is the number of membrane-contacting BR residues, and the second coordinate is the number of A-tail residues in contact with the BR. At low PIP_2 levels [Fig. 4(e), 0% PIP_2], the histogram corresponds to a single "closed-state" free-energy well, dominated by intramolecular contacts and little chance for membrane binding. As the PIP_2 level is increased to 20%, two states emerge: one is the closed state and the other is the semi-open state [Fig. 4(f)]. The energy barrier in between results from two divergent strategies for maximizing interactions by the BR, dominated by either intramolecular interactions (closed state) or intermolecular interactions (semi-open state). Note that the open state is not separated from but rather a sub-population of the semi-open state. At 30% PIP_2, the semi-open well broadens to flatten the energy barrier, and therefore, the energy landscape reverts to a single well [Fig. 4(g)]. An illustration of the changing energy landscapes at increasing PIP_2 is shown in Fig. 4(h).

Our major results for both the BR-only and BR-A fragments are in quantitative agreement with experimental data. For the BR-only fragment, the MD simulations show that membrane binding becomes substantial at 5% PIP_2 [Fig. 2(c)]. For the BR-A fragment, the MD simulations show that conformations competent for Arp2/3 binding become significantly populated around 15%–20% PIP_2 [Fig. 4(d)]. The 5% PIP_2 level for the BR-only is precisely the midpoint observed by Papayannopoulos *et al.*[3] in their membrane binding assay using a BR-GBD construct of N-WASP. The 15%–20% PIP_2 range for the BR-A fragment is also what is observed by these authors for the stimulation of Arp2/3-mediated actin polymerization by a BR-GBD-VCA construct.

Further support for the proposition that N-WASP starts to bind Arp2/3 even in the semi-open state comes from observations on Cdc42 in its activation of N-WASP. Both PIP_2 and Cdc42 alone can activate N-WASP, and the two together are synergistic.[3,7,12,16,17] Our previous MD study[18] found that Cdc42 competes against PIP_2 for binding the BR, especially its second half including Lys195, Arg 197, and Lys200. Here, we have found that the second half of the BR plays a major role in locking in the A tail; binding to the second half of the BR by Cdc42 will induce the release of the A tail, enabling its engagement with Arp2/3 and explaining how Cdc42 alone can activate N-WASP. Moreover, because both Cdc42 and PIP_2 facilitate A-tail release, their simultaneous presence will lead to not only a lower PIP_2 threshold for N-WASP activation but also synergistic activation.

The picture that emerges from our MD simulations is that N-WASP has the preponderance to stay autoinhibited, where it samples a variety of conformations stabilized by intramolecular interactions including between the BR and A motif that prevent Arp2/3 binding [Fig. 5(a)]. As PIP_2 increases to 15%–20% (or lower when Cdc42 is present), the semi-open state becomes stable, where the A tail is now free to engage with Arp2/3. The initial engagement primes Arp2/3 to pull the A motif away from the BR, leading to their full binding and, therefore, bypassing the need for first reaching the open state [Fig. 5(c)]. The pre-engagement with Arp2/3 by N-WASP in the semi-open state provides a functional rescue for a detrimentally low population of the open state.

SUPPLEMENTARY MATERIAL

See supplementary material for methods.

ACKNOWLEDGMENTS

This work was supported by the National Institutes of Health (Grant No. GM118091).

AUTHOR DECLARATIONS

Conflict of Interest

The authors have no conflicts to disclose.

Author Contributions

Souvik Dey: Data curation (lead); Formal analysis (equal); Investigation (equal); Methodology (lead); Visualization (lead). **Huan-Xiang Zhou**: Conceptualization (lead); Funding acquisition (lead); Investigation (equal); Project administration (lead); Supervision (lead); Writing – original draft (lead); Writing – review & editing (lead).

DATA AVAILABILITY

The data that support the findings of this study are available from the corresponding author upon reasonable request.

REFERENCES

[1] J. Monod, J. Wyman, and J.-P. Changeux, J. Mol. Biol. **12**, 88 (1965).
[2] X. Tang, S. Orlicky, T. Mittag, V. Csizmok, T. Pawson, J. D. Forman-Kay, F. Sicheri, and M. Tyers, Proc. Natl. Acad. Sci. U. S. A. **109**, 3287 (2012).
[3] V. Papayannopoulos, C. Co, K. E. Prehoda, S. Snapper, J. Taunton, and W. A. Lim, Mol. Cell **17**, 181 (2005).
[4] R. B. Berlow, H. J. Dyson, and P. E. Wright, J. Mol. Biol. **430**, 2309 (2018).
[5] L. M. Machesky and R. H. Insall, Curr. Biol. **8**, 1347 (1998).
[6] H. Miki and T. Takenawa, Biochem. Biophys. Res. Commun. **243**, 73 (1998).
[7] R. Rohatgi, L. Ma, H. Miki, M. Lopez, T. Kirchhausen, T. Takenawa, and M. W. Kirschner, Cell **97**, 221 (1999).
[8] J.-B. Marchand, D. A. Kaiser, T. D. Pollard, and H. N. Higgs, Nat. Cell Biol. **3**, 76 (2001).
[9] A. Zimmet, T. Van Eeuwen, M. Boczkowska, G. Rebowski, K. Murakami, and R. Dominguez, Sci. Adv. **6**, eaaz7651 (2020).
[10] H. Miki, T. Sasaki, Y. Takai, and T. Takenawa, Nature **391**, 93 (1998).
[11] A. S. Kim, L. T. Kakalis, N. Abdul-Manan, G. A. Liu, and M. K. Rosen, Nature **404**, 151 (2000).
[12] K. E. Prehoda, J. A. Scott, R. D. Mullins, and W. A. Lim, Science **290**, 801 (2000).
[13] S. B. Padrick and M. K. Rosen, Annu. Rev. Biochem. **79**, 707 (2010).
[14] L. Ou, M. Matthews, X. Pang, and H.-X. Zhou, FEBS J. **284**, 3381 (2017).
[15] D. Wu and H.-X. Zhou, Sci. Rep. **9**, 6172 (2019).
[16] R. Rohatgi, H.-y. H. Ho, and M. W. Kirschner, J. Cell Biol. **150**, 1299 (2000).
[17] N. Tomasevic, Z. Jia, A. Russell, T. Fujii, J. J. Hartman, S. Clancy, M. Wang, C. Beraud, K. W. Wood, and R. Sakowicz, Biochemistry **46**, 3494 (2007).
[18] S. Dey and H. X. Zhou, J. Mol. Biol. **435**, 168035 (2023).
[19] A. Hicks, C. A. Escobar, T. A. Cross, and H.-X. Zhou, JACS Au **1**, 66 (2021).
[20] S. Dey and H.-X. Zhou, J. Mol. Biol. **434**, 167817 (2022).
[21] S. T. Smrt, C. A. Escobar, S. Dey, T. A. Cross, and H. X. Zhou, "An Arg/Ala-rich helix in the N-terminal region of *M. tuberculosis* FtsQ is a potential membrane anchor of the Z-ring," Commun. Biol. (in press).
[22] M. Macainsh and H.-X. Zhou, Prot. Sci. **32**, e4581 (2023).
[23] J. A. Maier, C. Martinez, K. Kasavajhala, L. Wickstrom, K. E. Hauser, and C. Simmerling, J. Chem. Theory Comput. **11**, 3696 (2015).
[24] S. Piana, A. G. Donchev, P. Robustelli, and D. E. Shaw, J. Phys. Chem. B **119**, 5113 (2015).
[25] I. R. Gould, A. A. Skjevik, C. J. Dickson, B. D. Madej, and R. C. Walker, "Lipid17: A comprehensive AMBER force field for the simulation of zwitterionic and anionic lipids" (unpublished).
[26] R. Salomon-Ferrer, A. W. Götz, D. Poole, S. Le Grand, and R. C. Walker, J. Chem. Theory Comput. **9**, 3878 (2013).
[27] H.-X. Zhou, FEBS Lett. **552**, 160 (2003).